ACS Sustainable Chemistry & Engineering

Research Article

pubs.acs.org/journal/ascecg

Papain@Magnetic Nanocrystalline Cellulose Nanobiocatalyst: A Highly Efficient Biocatalyst for Dipeptide Biosynthesis in Deep Eutectic Solvents

Shi-Lin Cao,[†,‡] Hong Xu,[†] Xue-Hui Li,[†] Wen-Yong Lou,*[,‡,§] and Min-Hua Zong[†,§]

[†]School of Chemistry and Chemical Engineering, South China University of Technology, Guangzhou 510640, China

[‡]Lab of Applied Biocatalysis, School of Light Industry and Food Sciences, South China University of Technology, Guangzhou 510640, China

[§]State Key Laboratory of Pulp and Paper Engineering, South China University of Technology, Guangzhou 510640, China

Supporting Information

ABSTRACT: Magnetic nanocrystalline cellulose (MNCC), a novel biobased nanocomposite, was prepared via a simple coprecipitation-cross-linking technique and structurally characterized. Papain (PA) was successfully immobilized onto the MNCC. The resulting nanobiocatalyst PA@MNCC showed high PA loading (333 mg/g) and enzyme activity recovery (more than 80%). The stability of PA@MNCC was greatly superior to that of its free counterpart. Also, PA@MNCC manifested markedly enhanced solvent tolerance. The secondary structure study of the enzyme proved that these enhancements were attributed to the increase of structure rigidity of PA@MNCC. The observed optimum pH and temperature of PA@MNCC were significantly higher than the corresponding levels of free PA. A kinetic study demonstrated that PA@MNCC had an increase in enzyme-substrate affinity. Furthermore, the as-prepared PA@MNCC was successfully used as an efficient biocatalyst for the synthesis of *N*-(benzyloxycarbonyl)-alanyl-glutamine (Z-Ala-Gln) dipeptide in deep eutectic solvent (DES), choline chloride (ChCl):urea(1:2), with a high yield (about 71.5%), which, to our knowledge, was greatly higher than that reported previously. Besides, the novel PA@MNCC was easily recycled from the reaction medium by magnetic forces. Obviously, MNCC is a promising and competitive enzyme carrier and the as-prepared nanobiocatalyst PA@MNCC exhibited great potential for efficient biosynthesis of dipeptide.

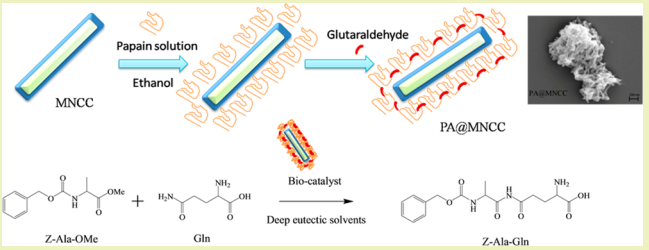

KEYWORDS: *Magnetic nanoparticle, Nanocrystalline cellulose, Dipiptide, Deep eutectic solvent, Protease, Green chemistry, Sustainable chemistry*

INTRODUCTION

Papain (PA), obtained from papaya latex, is a highly specific and effective biocatalyst and has been widely applied in the food industry.[1] However, soluble enzymes are unstable, as they are easy to denature or deactivate, and are difficult to recover and recycle. This prevents their further industrial application. Immobilization of free enzymes is an effective way of solving these problems. The ideal immobilization methodology should meet the following requirements: (i) The enzyme carrier should exhibit a high specific surface area, good biocompatibility, recycle easily and be capable of binding large amounts of enzyme with recovery of enzymatic activity. (ii) The immobilization process should be simple, rapid and mild. (iii) The immobilized enzyme should exhibit stability as well as promising industrial application.

Cellulose is one of the most abundant sources of renewable biopolymers.[2] It is of great interest to make full use of this eco-friendly and low-cost biomass feedstock to produce valuable chemicals,[3] biofuels[2] and biocompatible materials.[4] To date, use of cellulose as promising raw materials for production of biofuels and chemicals has been extensively studied. To our best knowledge, however, utilization of nanocrystalline cellulose (NCC) derived from cellulose as enzyme carriers has been far from fully explored. NCC is generally prepared by acid-catalyzed hydrolysis of cellulose,[5] and has drawn increasing attention due to its excellent physicochemical properties (including high surface-to-volume ratios, high aspect ratios, high stiffness, good strength) and sustainability.[6] Glucose oxidase,[7] peroxidase[8] and lysozyme,[9] as well as papain,[10] were successfully immobilized onto NCC with enhanced activity, stability and catalytic efficiency. This indicated that the novel NCC-based enzyme carriers show great potential and are worthy of further study. It is noteworthy that the stable dispersion of NCC in the reaction system prevented the recycling and further application of enzymes immobilized onto the NCC-based carrier.[10] Thus, the incorporation of magnetic

Received: April 11, 2015
Revised: June 3, 2015
Published: June 9, 2015

DOI: 10.1021/acssuschemeng.5b00290
ACS Sustainable Chem. Eng. 2015, 3, 1589−1599

Scheme 1. Schematic Representation for the Enzymatic Synthesis of Z-Ala-Gln

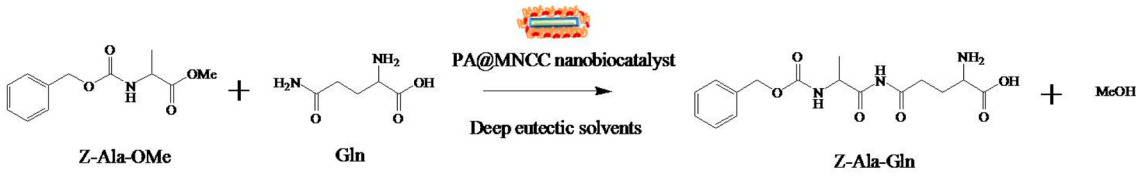

Fe_3O_4 nanoparticles (MNPs) into the NCC polymer matrix may be a potential method for obtaining a well dispersed and easily separated NCC-based nanomaterial. Recently, we prepared a novel biocompatible magnetic NCC (MNCC) composite via a simple coprecipitation-electrostatic-self-assembly technique and the results showed that the enzyme immobilized onto this novel MNCC showed enhanced stability and catalytic efficiency for biomacromolecule hydrolysis.[10] However, the amount of enzyme loaded onto the MNCC needs to be improved, and the immobilized enzymatic catalytic performance of the small molecules synthesized require further study. In addition, previous studies on NCC-immobilized enzymes focused on the aqueous phase of the enzymatic reaction system. Thus, it would be interesting to explore the application of the enzyme immobilized onto MNCC-based nanomaterials in other solvent systems.

Oligopeptides including dipeptides, used as functional food ingredients, play an important role in the food industry.[11] Among them, L-alanyl-L-glutamine (Ala-Gln) dipeptide is an important nutrient supplement[12] and can be used to prevent intestinal atrophy.[13] Besides, the Ala-Gln dipeptide is widely applied as an alternative to glutamine in medical fields due to its higher thermal stability and solubility.[14,15] Accordingly, there is an increasing need for a highly efficient synthesis of the valuable dipeptides. To date, three main technologies have been available for synthesis of dipeptide: chemical synthesis, cell fermentation and enzymatic synthesis. Enzymatic synthesis of dipeptides, using serine or cysteine proteases (such as papain) as biocatalysts, has become more favorable due to its mild catalytic conditions, minimum side-chain protection, and high stereospecificity.[16,17] To improve the efficiency of the enzymatic synthesis of dipeptides, different reaction media (such as aqueous solution,[18] ionic liquid,[19] frozen solution,[20] organic solvent,[21] as well as supercritical carbon dioxide) have been also employed. Recently, deep eutectic solvents (DESs) have emerged as promising green alternatives to conventional and unconventional solvents (such as ionic liquids) because of being much lower cost, more biodegradable and less toxic, and can be prepared simply through mixing an ammonium salt (such as choline chloride) and hydrogen bond donors (such as urea and glycerol).[22] As inexpensive, sustainable and biocompatible solvents, DESs have been successfully employed for biocatalytic processes with improved activity and stability of enzyme as well as minimized side effects.[23] Currently, Ala-Gln, a valuable dipeptide, is prepared mainly through a chemical synthesis method. To date, the enzymatic synthesis of Ala-Gln has been explored little, with only one account.[13] In this case, the protease-mediated synthesis of *N*-(benzyloxycarbonyl)-alanyl-glutamine (Z-Ala-Gln), a precursor of Ala-Gln, was conducted by using Z-Ala-OMe and Gln as an acyl donor and nucleophile, respectively, in aqueous buffer with a yield of about 35%. Generally speaking, it is of great interest to study the enzymatic synthesis of Z-Ala-Gln catalyzed of immobilized papain onto the novel MNCC support in a novel DES-containing system to improve further the dipeptide yield and the reaction efficiency.

In the present study, we describe, for the first time, the preparation of a novel MNCC via a simple coprecipitation-cross-linking technique and the use of this as-prepared material as the enzyme carrier for immobilization of papain (PA). Moreover, a comparative study of immobilized PA onto MNCC (PA@MNCC) and free PA showed that the PA@MNCC had significantly enhanced stability and catalytic efficiency. Furthermore, the green and biocompatible DES, ChCl:urea (1:2), was employed, for the first time, as the reaction medium for efficient enzymatic synthesis of Z-Ala-Gln from Z-Ala-OMe and Gln with a satisfactory yield of more than 71% using the as-prepared PA@MNCC (Scheme 1). Also, the effects of several crucial variables on the enzymatic synthesis of Z-Ala-Gln were here discussed.

EXPERIMENTAL SECTION

Preparation of Magnetic Nanocrystalline Cellulose (MNCC). Nanocrystalline cellulose was isolated from microcrystalline cellulose according to the method of Bondeson described in detail elsewhere.[24,25] The conditions of MNCC synthesis are shown in Table S1 of the Supporting Information. Given amounts of ferrous chloride tetrahydrate (5.36 g), ferric chloride hexahydrate (13.6 g) and chitosan (0.6) were thoroughly dissolved in a 1.5 wt % NCC aqueous suspension. Then, ammonium hydroxide (28%, w/w) was added under continuous stirring at 40 °C for 30 min. Then, epichlorohydrin was added to the mixture, and the mixture was incubated for 90 min at 80 °C. The resulting precipitate was washed with distilled water for 5 times and subjected to magnetic separation using a magnetic field. These collected MNCC materials were stored as stock suspensions with a solid content of 2% (w/v) prior to use.

Immobilization of PA on the Activated MNCC (PA@MNCC). The prepared MNCC was first activated with L-cysteine as described below.[26] The activated MNCC were stored at 4 °C, and isolated by magnetic decantation and washed with methanol (2 × 10 mL) and water (2 × 10 mL) prior to use. These materials were stored as the stock suspensions with a solid content of 2%. The immobilized PA onto MNCC (PA@MNCC) was prepared as follows. The activated MNCC was mixed with free enzyme in PBS (50 mM, pH 7.0) under magnetic stirring for 30 min at 4 °C. Then, water-free ethanol was added into the above mixture to precipitate the enzyme for 10 min under stirring, followed by injecting a given amount of 25% glutaraldehyde (GA) and stirring for 120 min. After cross-linking, PA@MNCC was washed for at least 3 times with PBS (50 mM, pH 7.0) and stored at 4 °C for subsequent use. The immobilization conditions of the enzyme onto the prepared MNCC support including mass ratio of PA to MNCC, GA mass fraction and cross-linking time have been optimized through single factor experiment. The immobilization process is shown in Scheme S1 of the Supporting Information.

Enzyme Activity Assay. The catalytic activity of PA@MNCC was assayed by PA-mediated degradation of *N*-α-benzoyl-D,L-arginine-*p*-nitroanilide (BAPNA).[27] Free PA or PA@MNCC (2.0 mg) was dispersed into 2 mL of phosphate buffer (50 mM, pH 7.0), and incubated at 40 °C for 5 min. The reaction was then initiated by adding 1 mL of substrate solution containing 0.9198 mM BAPNA. The concentration of *p*-nitroaniline (*p*NA) released was detected over

DOI: 10.1021/acssuschemeng.5b00290
ACS Sustainable Chem. Eng. 2015, 3, 1589−1599

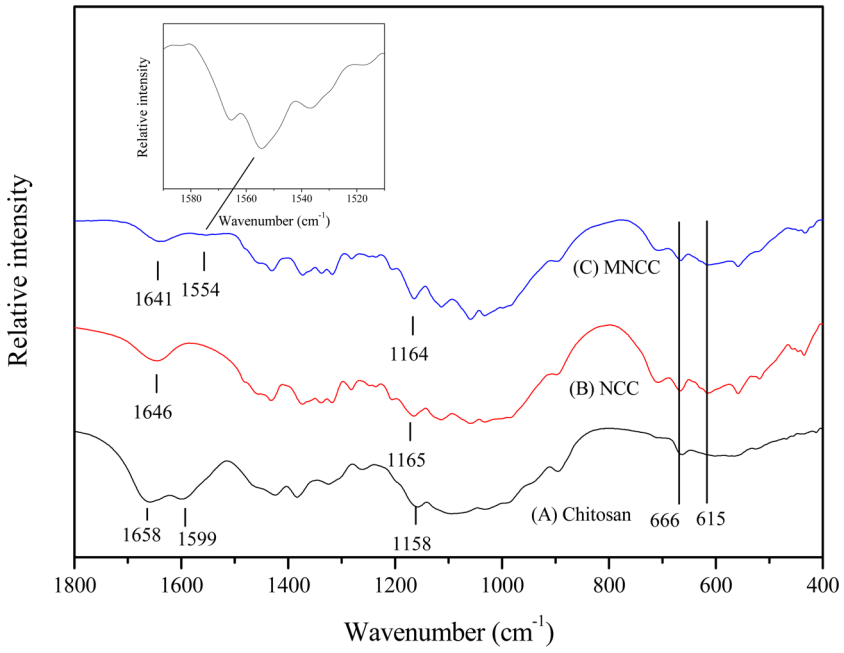

Figure 1. FTIR spectra for chitosan (A), NCC (B) and MNCC-6 (C).

10 min at 405 nm against a blank sample without enzyme. One unit of enzyme activity was defined as the amount of the formed *p*NA (pmol) with 1.0 mg of enzyme per min. The enzyme activity recovery of PA@MNCC was calculated as the ratio of PA@MNCC activity to that of the same amount of free PA.

General Procedure for the PA-Catalyzed Synthesis of Z-Ala-Gln in ChCl:urea (1:2) DES. The deep eutectic solvent (DES), ChCl:urea (1:2) (CU-DES), was prepared following Abbott's method.[22] In a typical experiment, the cosolvent system of CU-DES (1.5 mL) and water (0.3 mL) containing 30 mg (0.2055 mmol) of Gln and 0.14 mL of triethylamine (TEA) was added to a 10 mL Erlenmeyer flask capped with a septum, and subsequently 23.73 mg (0.1 mmol) of Z-Ala-OMe in 0.1 mL of ethanol was added to the mixture. The enzymatic reaction of Z-Ala-Gln synthesis was initiated by 367U free PA or PA@MNCC at 50 °C and a stirring rate of 200 r/min. Samples (0.1 mL) were withdrawn at specified time intervals from the reaction system, and then 0.1 mL of 12 M HCl was added to quench the enzymatic reaction and diluted with elution solution (35% acetonitrile in distilled water with 0.1% trifluoroacetic acid) prior to HPLC analysis. The detailed HPLC analysis is shown in the Supporting Information.

RESULTS AND DISSCUSSION

Preparation and Characterization of MNCC. The FTIR spectra displayed in Figure 1 were recorded to confirm the chemical composition of the nanocomposite. The peaks at 1658 and 1599 cm^{-1} were identified as the amide I and II groups of chitosan (Figure 1A).[28] The vibrational frequency at approximately 615 cm^{-1} was the β-glycosidic linkages of the sugar units. Bending signals at 1165 and 1114 cm^{-1} were typical frequencies of C−O−C and an asymmetrical ring, respectively, and absorption peaks at about 666 and 615 cm^{-1} were due to C−C−O and C−OH, respectively, and were peaks of the NCC (Figure 1B).[29] It is noteworthy that in the MNCC spectra (Figure 1C), the bands at 1599 cm^{-1} became weaker, and this may have been attributed to the strong hydrogen bonding between the NCC, chitosan and Fe_3O_4.[30] Moreover, the chitosan characteristic peak of ($CONH_2$) at 1659 cm^{-1} shifted to 1641 cm^{-1} and a considerably weaker peak shift from 1599 to 1554 cm^{-1} (which was due to amide II groups), indicated that the epichlorohydrin preferred to cross-link with the hydroxy group of the polysaccharide rather than amide II groups of the chitosan via covalent bonds.[31] The C−O−C stretch vibration at about 1165 cm^{-1} in the spectra of NCC as well as the absorption at 1158 cm^{-1} for chitosan shifted to 1164 cm^{-1} in the MNCC spectra, demonstrating that the NCC interacted with both chitosan and Fe_3O_4.

The diffractions from NCC (Figure 2B) and MNCC (Figure 2D−F) were resolved into peaks at 14.8°, 16.5°, 22.7° and

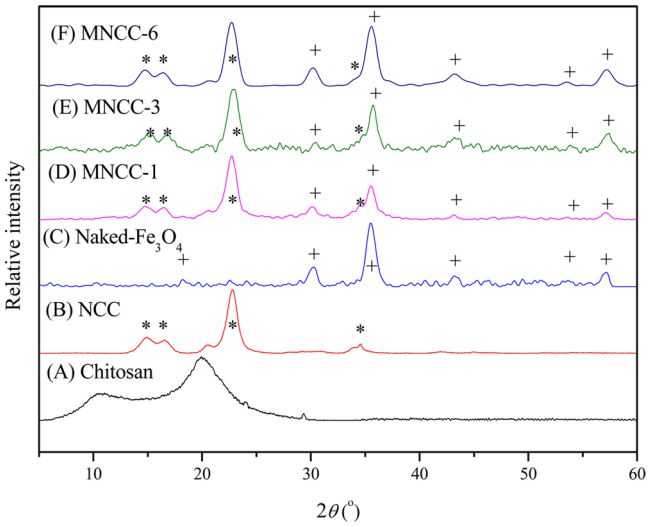

Figure 2. XRD spectra for chitosan (A), NCC (B), naked Fe_3O_4 (C), MNCC-1 (D), MNCC-3 (E) and MNCC-6 (F).

34.5° and assigned to the crystallographic planes of (101), (10−1), (002) and (040),[32] respectively. The first three peaks (2θ = 14.8°, 16.5° and 22.7°) were characteristic peaks for the cellulose I structure,[9] demonstrating that during both preparation processes, the crystalline structure of cellulose was maintained. The (101) lattice planes were identified as amorphous, and the (002) lattice planes were crystalline zone

DOI: 10.1021/acssuschemeng.5b00290
ACS Sustainable Chem. Eng. 2015, 3, 1589−1599

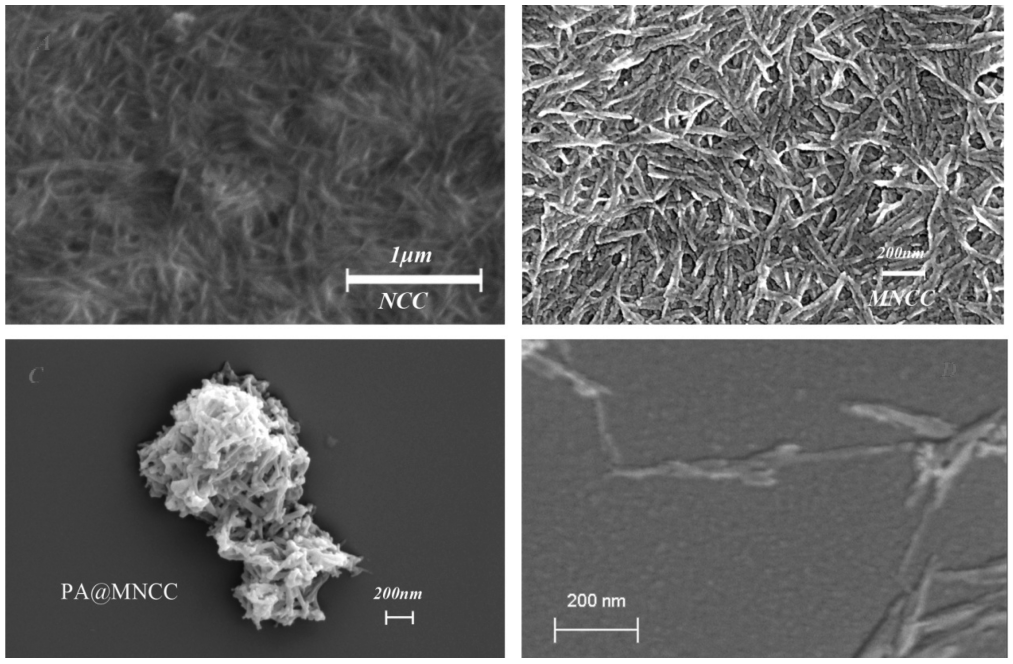

Figure 3. SEM analysis of NCC (A), MNCC (B, D) and PA@MNCC (C).

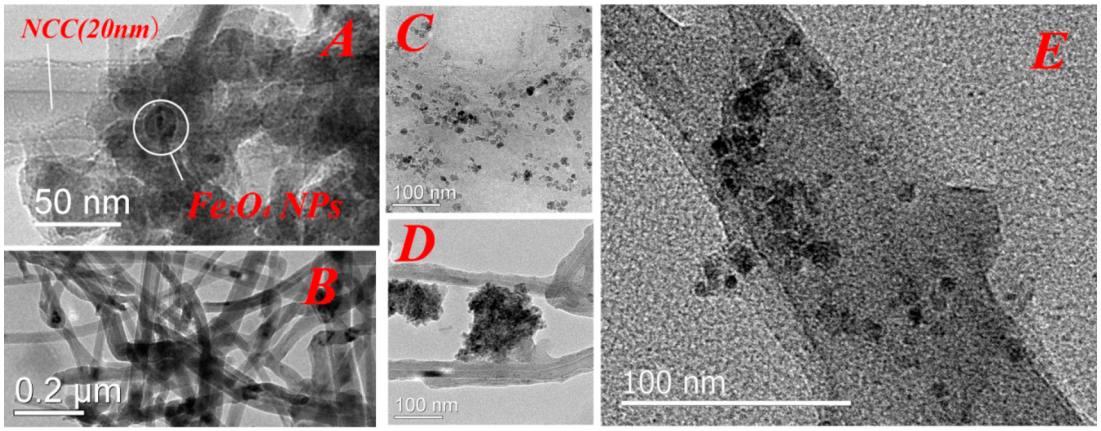

Figure 4. TEM analysis of the MNCC (A, B), the magnetic NPs prepared in the absence of NCC (C), a comparative coprecipitation process with epichlorohydrin cross-linker (D) and PA@MNCC (E).

diffractions. The high degree of crystallinity of chitosan (Figure 2A) was illustrated by the two strong peaks at 10.5° and 20.2°.[33] Moreover, the crystallinity index (CI) value of chitosan was 54.2%. Also, the CI value of CNC was about 73.9%. However, the characteristic peak at 10.5° (chitosan) disappeared at the diffractions of MNCC (Figure 2D), indicating that chitosan formed a network structure of interpenetrating polysaccharides cross-linked with each other by epichlorohydrin.[31] The strong and distinct diffraction peak of magnetic Fe_3O_4 (Figure 2C) was recorded for MNCC (Figure 2D), confirming the presence of magnetic Fe_3O_4 (JCPDS card No. 19-0629) with the peaks at 2θ = 18.2−18.5° (111), 30−31° (220), 35−36° (311), 43−43.5° (400), 53−53.5° (422) and 57° (511).

The saturated magnetizations (M_s) of the prepared eight MNCCs under different conditions (Table S1 in Supporting Information) were determined, and are summarized in Table S2 of the Supporting Information. The highest M_s value of MNCC was observed at MNCC-6 with a value of 10.10 emu/g. The M_s values of the materials were significantly affected by the mass fraction of the magnetic iron oxides. In addition, according to the findings in Table S2 of the Supporting Information (MNCC-6−8), the M_s of the Fe_3O_4 NPs decreased with increased amounts of chitosan. This was due to the small quantity of chitosan that tightly encapsulated the Fe_3O_4 NPs on the surface of the NCC matrix to inhibit the grain size of the crystalline MNPs, and thus decreased the M_s of the tri-iron tetroxide.[34] As shown in Figure S1 of the Supporting Information, the MNCC-6 with the highest M_s value was easily attracted and separated from the mixture by an external magnetic field, and it took about 10 s to recover fully the immobilized enzyme onto MNCC-6 (PA@MNCC).

On the basis of elemental analysis, the contents of Fe_3O_4, chitosan and NCC in the prepared MNCC (unless otherwise specified, MNCC corresponds to MNCC-6 in this work) were calculated to be 45.7 wt % (5.96 g), 4.1 wt % (0.54 g) and 50.2 wt % (6.54 g), respectively. Surprisingly, no significant loss of Fe_3O_4 (less than 1% (0.1 g)) was observed during the preparation process of MNCC according to the determined content of Fe_3O_4, in the final materials, suggesting that the used

DOI: 10.1021/acssuschemeng.5b00290
ACS Sustainable Chem. Eng. 2015, 3, 1589−1599

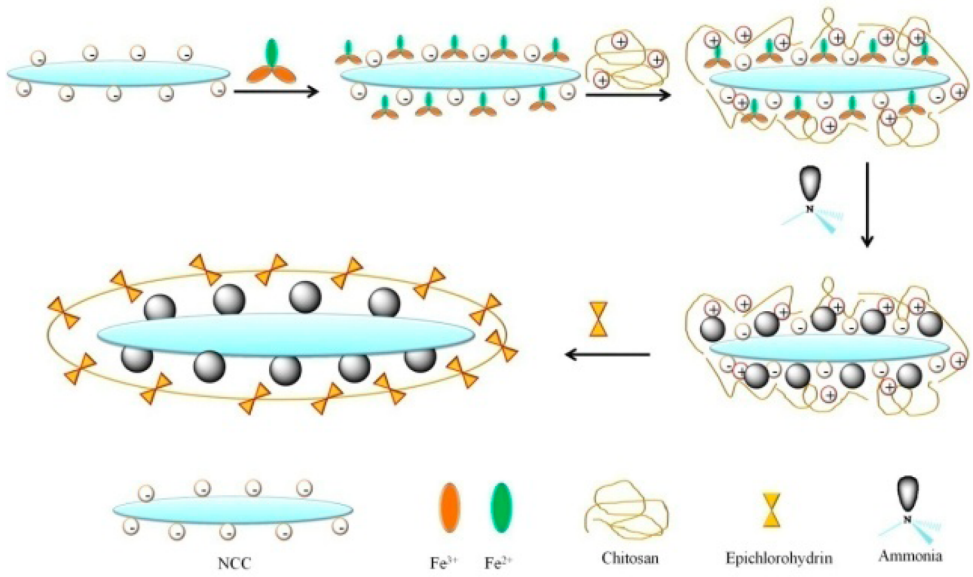

Figure 5. Schematic representation for the synthesis of MNCC.

Fe_3O_4 was almost fully loaded onto NCC. On the other hand, the contents of the raw materials for NCC and chitosan were 51.6 wt % (7.00 g) and 4.4 wt % (0.60 g), whereas those of the final products were recorded around 50.2 wt % (6.54 g) and 4.1 wt % (0.54 g), respectively. Therefore, the prepared MNCC could be readily separated and purified from the mixture including the residual NCC and chitosan by a magnetic field.

The thermal stability of NCC, chitosan and MNCC was measured by thermogravimetric analysis (TGA) under N_2 at a heating rate of 10 °C/min. The TGA plot in Figure S2 of the Supporting Information illustrates that NCC showed a weight loss of 67% between 210 and 320 °C and chitosan showed a weight loss of 50% at 240−400 °C. The weight loss for MNCC-6 between 295 and 420 °C was about 40%. Compared to NCC, the thermal onset of the decomposition of MNCC was shifted from 210 to 295 °C, indicating that Fe_3O_4 NPs significantly enhanced the thermal stability of NCC.

Figure 3 shows SEM micrographs of NCC and MNCC. The prepared NCC (Figure 3A) had a rod-like structure with a width of about 20 nm and that of MNCC (Figure 3B,D) was about 50 nm. Also, both length of NCC and MNCC was no more than 1000 nm. According to previous research, the size of NCC varied according to the types of raw materials used and the preparation conditions. Most of these types of nanomaterials are whisker-like materials with a width of 3−100 nm and length of 25−3000 nm.[6] Therefore, the NCC and MNCC materials in the present study conform to the definition of cellulose nanocrystal materials. The rod-like PA@MNCC aggregated together after drying is clearly seen at Figure 3C, and consequently showed the relatively big size of about 600 nm. To obtain the accurate size of single PA@MNCC, we have reprepared the sample and reperformed TEM analysis for PA@MNCC. The width of single PA@MNCC was found to be about 80 nm (Figure 4E).

TEM analysis of the prepared MNCC (The CNC/Fe_3O_4 ratio is 1.097/1 (g/g)) is shown in Figure 4. Figure 4A,B confirms the stable and homogeneous dispersion of Fe_3O_4 NPs on the surface of NCC and the uniform chitosan coating. The size of the Fe_3O_4 NPs was less than 20 nm. Furthermore, the magnetic NPs prepared in the absence of NCC were a similar size (10−20 nm) (Figure 4C), suggesting that the NCC did not significantly affect the size of Fe_3O_4 NPs coated with chitosan bound on the surface of the NCC. To investigate whether the chitosan-coated Fe_3O_4 NPs were composited without NCC by cross-linking or physical absorption, a comparative coprecipitation process with epichlorohydrin cross-linker was carried out. As is shown in Figure 4D, without a cross-linker, the chitosan-coated Fe_3O_4 NPs aggregate with each other and fail to disperse homogeneously onto the surface of NCC. This result clearly proved that the chitosan coated Fe_3O_4 NPs were composited with NCC via epichlorohydrin cross-linking process.

The above results, especially the TEM result of the comparative study, strongly confirm the fabrication mechanism of MNCC. As depicted in Figure 5, MNCC was prepared *in situ* by a simple coprecipitation-cross-linking process. Initially, both Fe^{2+} and Fe^{3+} ions were absorbed by NCC. Subsequently, chitosan, carrying abundant positively charged amino groups ($-NH_2$), was chelated with both Fe^{2+} and Fe^{3+} ions[35] and coated onto the surface of NCC.[36] When ammonia was added to the mixture, black-colored Fe_3O_4 NPs were formed. Following the addition of epichlorohydrin, chitosan cross-linked with each other to form a dense and disarry shell and tightly encapsulated the Fe_3O_4 NPs on the NCC matrix.

Immobilization of Papain on MNCC and Its Characteristics. The rationale to immobilized PA onto MNCC was a two-step process (Scheme S1 of the Supporting Information). First, the MNCC support was dispersed in the PA solution and then the PA was deposited on the surface of MNCC by adding ethanol as the precipitant. In the second step, glutaraldehyde was added and the PA protein was cross-linked and tightly coated on the surface of MNCC to finally form PA@MNCC.

Additionally, a comparative study has been made of the immobilization of PA on MNCC and Fe_3O_4 nanoparticles coated with chitosan (without NCC). It was found that the activity recovery of PA immobilized on Fe_3O_4 nanoparticles coated with chitosan was only 55.2% (7.5 U/mg support), which was remarkably lower than that of PA@MNCC-6 (80.1%, 10.9 U/mg support). This might be mainly attributable to the abundant active −OH groups of NCC that contribute to

DOI: 10.1021/acssuschemeng.5b00290
ACS Sustainable Chem. Eng. 2015, 3, 1589−1599

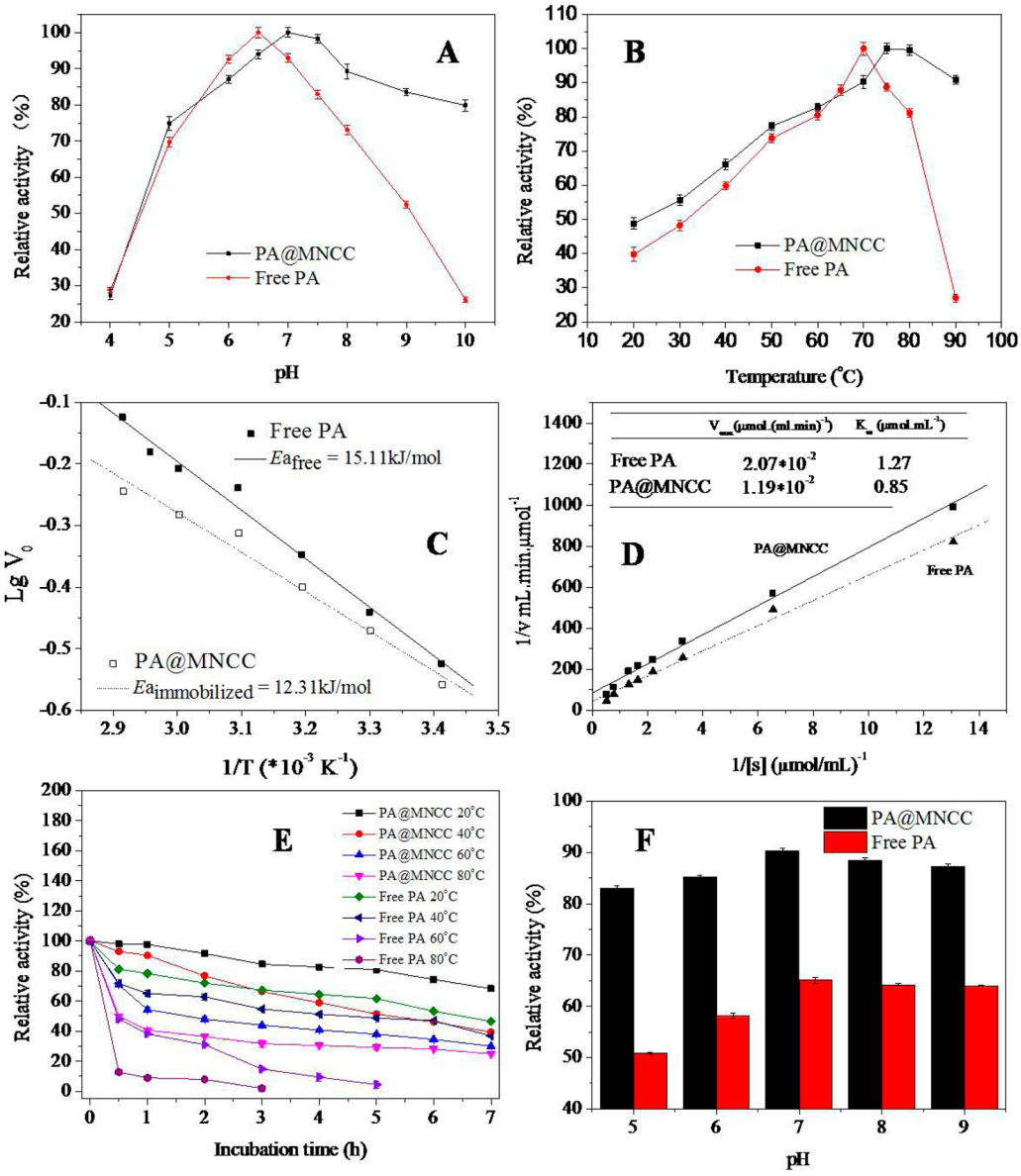

Figure 6. Enzymatic properties of free PA and PA@MNCC: (A) effect of pH on the PA@MNCC (■) and free PA (○); (B) effect of temperature on the PA@MNCC (■) and free PA (○); (C) apparent activation energy of PA@MNCC and free PA; (D) kinetics behaviors of free PA and PA@MNCC; (E) thermal stability of free PA and PA@MNCC; (F) pH stability of free PA and PA@MNCC.

the cross-linking of PA on the MNCC. Obviously, NCC plays a key role in PA immobilized onto MNCC with enhanced activity recovery and catalytic performance.

PA was mixed with MNCC at different mass ratios (PA/MNCC, 1:0, 1:1, 1:2, 1:2.5, 1:3, 1:3.5, 1:4, 1:8) in phosphate buffer (50 mM, pH 7.0) and then precipitated onto the surface of MNCC by adding 10-fold nonaqueous ethanol. The resultant sediments (without glutaraldehyde (GA) addition) were collected for enzyme activity assay (Figure S3 in the Supporting Information). Of all the examined mass ratios of PA to MNCC, the highest enzyme activity recovery recorded 85.6% at a ratio of 1/3, which was considered as the most suitable one for PA precipitation and recovery. Upon the addition of GA (around 1.92 wt %) to immobilize tightly PA on MNCC by cross-linking for 2.0 h, the observed enzyme activity recover decreased slightly from 85.6% to 80.1%, probably because of the partial inactivation of PA caused by GA attacking the active sites of enzyme. As expected, the concentration of GA and the cross-linking time affected significantly the enzyme activity recovery, and these effects were subsequently investigated.

As shown in Figure S4A of the Supporting Information, the activity recovery of PA@MNCC increased from 70.8% to 80.1%, with the GA mass fraction from 1.11% to 1.92% and the optimal GA mass fraction was approximately 1.92%, with an activity recovery of 80.1%. Also, although the GA mass fraction was higher than 1.92%, the activity recovery decreased to 78.8%. Moreover, the optimal cross-linking time was approximately 2.0 h (Figure S4B of the Supporting Information). Increasing both the GA mass fraction and cross-linking time decreased the enzyme activity. During enzyme immobilization, GA was used as a cross-linking agent and an enzyme inactivation agent, which can attack the active sites of the enzyme. In this study, PA@MNCC was prepared using the following typical conditions: 1.5 mg of PA was incubated with 4.5 mg of MNCC in 0.5 mL of pH 7.0 PBS at 0

DOI: 10.1021/acssuschemeng.5b00290
ACS Sustainable Chem. Eng. 2015, 3, 1589−1599

°C and then precipitated with 7.5 mL of anhydrous alcohol and cross-linked with 1.92% GA for 2 h. The amount of PA loaded onto the carrier was approximately 333 mg/g MNCC (this MNCC contained 45.7 wt % Fe_3O_4, 4.1 wt % chitosan and 50.2 wt % NCC), which is an almost 2-fold improvement compared with previously reported studies.[37] In addition, enzyme activity recovery was approximately 80.1%, and this value was a significant improvement compared with our previous study.[10]

The effect of pH on the enzymes is shown in Figure 6A. The optimal pH value for free enzyme was observed to be 6.5, but that of PA@MNCC was 7.0 (Figure 6A). As described previously, the cross-linking between GA and the basic residues of enzymes, such as tyrosinase,[38] lipase,[39] α-amylase[40] and acetyl xylan esterase,[41] changed the acidic or basic amino acid side chain ionization in the microenvironment around the catalytic site of the enzyme or the surface groups of MNCC. In addition, immobilized PA retained higher relative activity (>90%) above pH 7.0 compared with free PA, which demonstrated that immobilization prevented the enzyme from deactivating in alkaline conditions.

The effect of temperature on the enzymes is shown in Figure 6B. The optimum temperature for the highest PA activity was 70 °C for free enzyme and shifted to 75 °C for PA@MNCC (Figure 6B). The change in optimal temperature was attributed to an increase in the enzyme conformational rigidity (seen in secondary structure study below) and an improvement in PA heat resistance after covalent bond formation among proteins via GA cross-linking during the immobilization process.[40,42] It is noteworthy that PA@MNCC retained more than 90.9% of its relative activity in the temperature range of 75 to 90 °C, whereas the corresponding value for its free counterpart was approximately 29.9%. This good adaption of high temperature might be due to the prevention of autolysis of the enzyme after being immobilized onto MNCC. Similar results were also found by another research group.[43]

In addition, a comparative study was made of the apparent activation energy (E_a) of PA@MNCC and free PA-catalyzed hydrolysis of *N*-α-benzoyl-D,L-arginine-*p*-nitroanilide as a model reaction. As depicted in Figure 6C, the E_a value for PA@MNCC (12.31 ± 0.16 kJ/mol) was significantly lower than that for free PA (15.11 ± 0.08 kJ/mol). This result indicated that PA immobilized on MNCC had a lower sensitivity to temperature and made the formation of the transition state "enzyme-substrate" easier, possibly due to a significantly enhanced "enzyme-substrate" affinity[44] that was demonstrated by subsequent kinetic study for PA@MNCC.

The kinetic behaviors of free PA and PA@MNCC were compared (Figure 6D). It was found that the PA-mediated hydrolysis of BAPNA followed the Michaelis−Menten equation. The apparent V_{max} for free and immobilized PA was 2.07×10^{-2} and 1.19×10^{-2} μmol·(mL·min)$^{-1}$, respectively. The apparent kinetic parameter K_m for PA@MNCC was 0.85 μmol·mL^{-1}, which was lower than that for free PA (1.27 μmol·mL^{-1}), demonstrating the increase in enzyme-substrate affinity of PA@MNCC. The increase of the enzyme-substrate affinity after immobilization, indicated by the decrease of the K_m value, was possibly be attributable to one or more of the following reasons: (1) the prepared MNCC has the high specific surface area and the enzyme is anchored on the surface of MNCC, making the substrate accessible to the enzyme and thus increasing the apparent affinity, which is in accordance with a previous report;[45] (2) the immobilization of PA onto the MNCC may result in the conformational changes, helping the enzyme to orient suitably its active site toward the substrate, which can be supported by similar studies.[46,47]

The thermal stabilities of free PA and PA@MNCC were studied following incubation in phosphate buffer solution at different temperatures for 1−7 h. The residual activities are shown in Figure 6E. In general, the relative activities of both free PA and PA@MNCC decreased sharply when the incubation temperature increased from 20 to 80 °C. Comparing free PA and PA@MNCC at the same temperature, PA@MNCC exhibited higher thermal stability than its free counterpart. PA@MNCC retained more than 30% of its initial activity after 7 h of incubation at 80 °C, whereas free PA was inactivated after just 3 h of incubation. Moreover, when PA@MNCC was stored at 4 °C for 30 days, no significant loss of enzyme activity was seen.

To investigate the stability of PA@MNCC at different pH levels, the enzyme was incubated at 40 °C in phosphate buffer (50 mM) at pH 5−9 for 1 h (Figure 6F). PA@MNCC retained more than 83.1% of its initial activity, whereas the initial activity of free PA was approximately 50.8%. This indicated that PA@MNCC had much higher pH stability than free PA. Furthermore, these results also showed that both PA@MNCC and free PA were more stable in the pH range of 7−9 (neutral and alkaline conditions) than pH 5−6 (weak acidic conditions).[10]

In general, PA@MNCC showed significantly better solvent tolerance to all three solvents compared with its free counterpart (Figure S5A of the Supporting Information). *N*-Butyl alcohol and CU-DES showed the lowest toxicity to PA@MNCC. It is worth noting that free PA was significantly deactivated by two ionic liquids ([Bmim]I and [Amim]BF_4) and the residual activity was 58.6% and 60.4%, respectively. However, the residual activities of PA@MNCC in these ionic liquids were both more than 77%. Previous research showed that organic solvents and ionic liquids can damage the native structure of the enzyme, strip off protein-bound water, and result in rapid deactivation of the enzyme.[46] Due to immobilization, PA@MNCC maintained its catalytic conformation and exhibited more structural rigidity, resulting in greatly enhanced solvent tolerance after immobilization, which was in good agreement with previous reports.[48,49] To understand further the enhanced solvent tolerance of PA@MNCC, the secondary structural changes of PA@MNCC and free PA before and after 2 h of exposure to solvents were comparatively investigated by FTIR analysis, which is generally used method for the secondary structure of enzyme.[50] As shown in Figure S5B of the Supporting Information, only a slight decrease in the content of α-helix structure (from 28.97% to 28.68%) and β-sheet structure (from 11.38% to 11.09%) was observed with PA@MNCC after 2 h of exposure to CU-DES, whereas the contents of α-helix structure (from 23.35% to 20.24%) and β-sheet structure (from 11.20% to 7.22%) for free PA was markedly reduced. Besides, the corresponding increased content of random coil structure in PA@MNCC was much lower than that in free PA (around 2.3% vs 10.2%). Obviously, PA@MNCC maintained better the structural integrity and catalytic conformation after exposure to CU-DES than free PA, thus boosting the ability to solvent tolerance.

The reusability of PA@MNCC is a key factor in its low-cost utilization. The reusability of PA@MNCC was tested in up to 6 cycles. The initial and recovered activities of PA@MNCC for each cycle were 100%, 99.7%, 87.6%, 79.1%, 57.8% and 52.4%, respectively.

DOI: 10.1021/acssuschemeng.5b00290
ACS Sustainable Chem. Eng. 2015, 3, 1589−1599

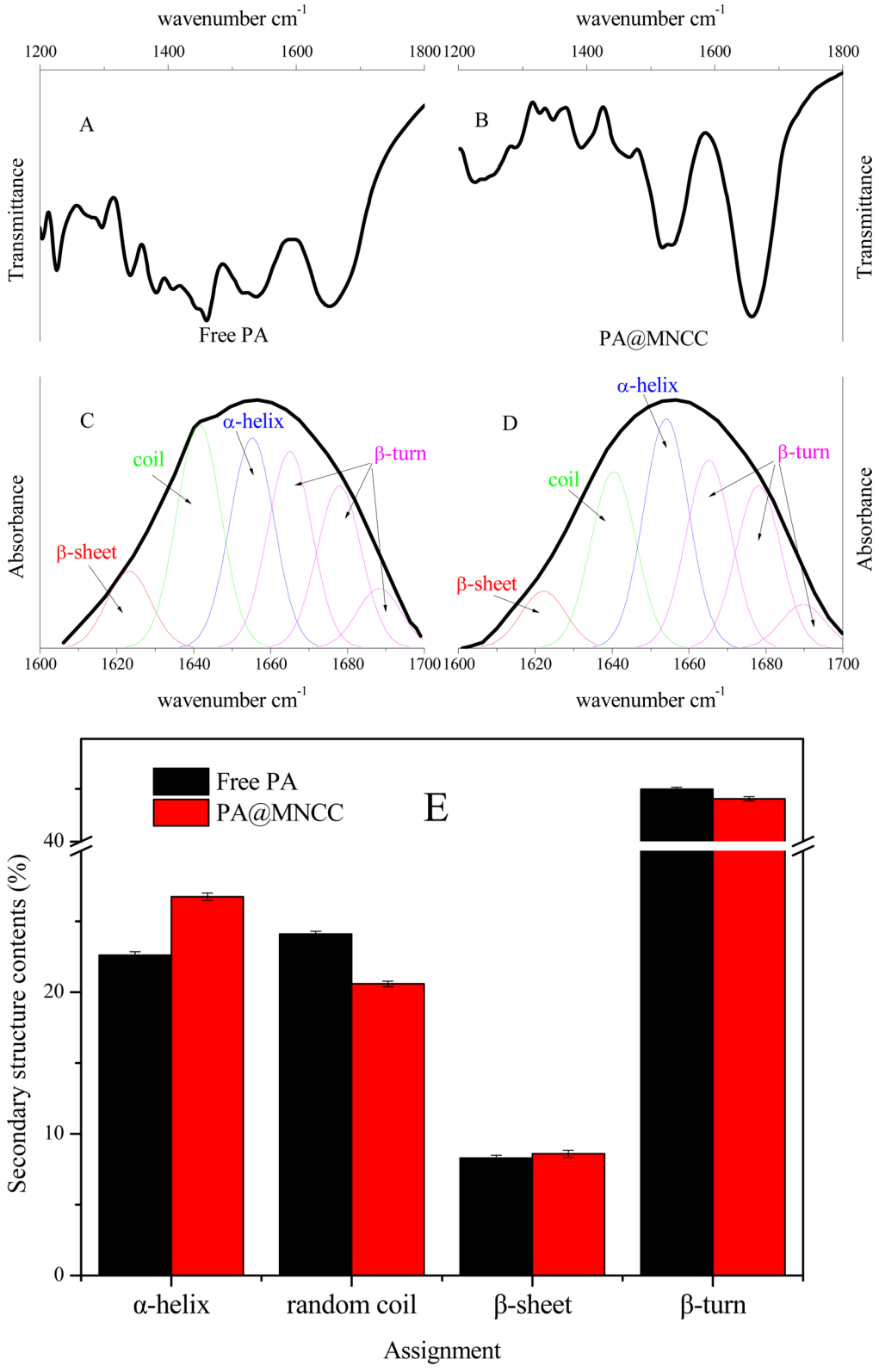

Figure 7. FTIR absorption spectrum of free PA (A) and PA@MNCC (B); amide I fitting results of free PA (C) and PA@MNCC (D); secondary sturctures changes of free PA and PA@MNCC (E) (black and other color lines indicate the experimental data and individual Gaussian components, respectively).

FTIR spectroscopy data analysis is a powerful way of the determination of the secondary structure of enzyme. Previous studies showed that the secondary structure contents of the enzyme can be obtained via the analysis of the amide I peak data (from 1600 to 1700 cm^{-1}). The amide I band originates from the C═O vibration of the enzyme chain. Moreover, the frequency of this band based on both hydrogen-bonding and coupling along the enzyme chain. Therefore, the amide I band

DOI: 10.1021/acssuschemeng.5b00290
ACS Sustainable Chem. Eng. 2015, 3, 1589−1599

is sensitive to the enzyme conformation.[51] Indeed, the conformation-catalystic performance relationships of protease have been successfully studied by FTIR analysis by our research group[52] as well as others.[53] The FTIR spectra were acquired with free PA as well as PA@MNCC (Figure 7A−D). For both free PA PA@MNCC, the bands at 1622−1623 cm^{-1} can be assigned to the β-sheet structure of the protein. The 1640−1641 cm^{-1} component can instead be attributed to the random coil structure. The α-helix structure component can be observed at 1654−1655 cm^{-1}. Furthermore, the bands around 1665−1690 cm^{-1}, can be assigned to β-turns. The conformation of both PA and PA@MNCC was summarized in Figure 7E. It is noteworthy that the α-helix content of PA@MNCC was significantly higher than that of free PA (26.80 ± 0.25% vs 22.67 ± 0.19%). Moreover, it should be noted that the random coil content of the PA@MNCC was around 20.65 ± 0.20% and this is 3.51% lower than that of its free counterpart. The strong hydrogen bonding or charge interactions play an important role in maintaining the conformation of α-helix structure as well as the structure rigidity and stability of the enzyme molecules.[54] Moreover, the structure rigidity of enzyme was necessary for the stabilities (thermal stability, pH stability, as well as organic solvent tolerance) of enzyme and the catalytic activity.[55−57] In the present study, the enhanced stabilities of PA@MNCC could be explained as follows: after being immobilized onto MNCC, the α-helix content of the enzyme increased and the random coil structure of the enzyme reduced, so that the structure rigidity and stability of enzyme molecules was improved.

PA@MNCC-Catalyzed Biosynthesis of Z-Ala-Gln in DES. As observed in Figure S6A of the Supporting Information, for both PA and PA@MNCC, lower amounts of water (approximately 5% v/v) led to a low yield of Z-Ala-Gln in ChCl:urea medium, illustrating denaturation of the enzyme under extremely dry conditions. Remarkably, the optimal water content for free PA and PA@MNCC was approximately 16% and 10% of water (v/v), respectively, and the peptide Z-Ala-Gln was obtained in a 62.53% and 66.28% yield, respectively. These results indicated that immobilized PA (PA@MNCC) exhibited higher catalytic efficiency at lower water content than free PA. For both PA@MNCC and free PA, a favorable yield of Z-Ala-Gln was observed when the water content (v/v) in the solution was between 15% and 22%. Previous literature showed that water content in the range of 10−25% v/v was suitable for enzymatic synthesis of protected *N*-Ac-Phe-Gly-NH_2 dipeptide and prevented hydrolysis of the substrate *N*-acetylphenylalanine ethyl ester.[58]

In this study, the biosynthesis of Z-Ala-Gln is a nucleophilic reaction.[16] PA acts as a transferase and forms an acyl-enzyme intermediate. As shown in Figure S6B of the Supporting Information, with increased KCl concentration the yield of Z-Ala-Gln catalyzed by free PA and/or PA@MNCC decreased by 18% and 8%, respectively. This decrease was mainly caused by high ionic strength, which changed the affinity of PA to the Z-Ala-OMe substrate and led to a lower yield.[13,59] Moreover, it should be noted that the yield of PA@MNCC catalytic Z-Ala-Gln synthesis was approximately 58.6%, which was about 10% higher than the yield catalyzed by its free counterpart. These results also indicated an increase in the enzyme-substrate affinity of PA@MNCC, which corresponded to the kinetic behavior of PA@MNCC observed in the present study.

Temperature is also an important reaction parameter that significantly influences the yield of enzymatic dipeptide synthesis. As depicted in Figure S6C of the Supporting Information, the highest dipeptide yield was observed at 50 °C for both free PA and PA@MNCC, which was lower than the optimal temperature for PA activity in BAEE hydrolysis in this study. Similar results were observed previously.[13] With an increase in temperature from 50 to 70 °C, the yield of Z-Ala-Gln catalyzed by free PA sharply decreased to about 15%, whereas the yield in the PA@MNCC-catalyzed reaction was more that 50%. According to the pH profiles and the E_a of both free PA and PA@MNCC, these results were mainly due to a decline in enzyme conformational flexibility, and stabilization of the three-dimensional structure of the transformed enzyme, as well as the transition state intermediate after immobilization of PA onto MNCC.

The substrate ratio between the nucleophile Gln and acyl donor Z-Ala-OMe (G/Z ratio) affected the yield of dipeptide synthesis. In this nucleophilic reaction, both H_2O and Gln can react with the Z-Ala-enzyme intermediate (ZAE). Thus, increasing the G/Z ratio resulted in ZAE forming the final product, Z-Ala-Gln, instead of the side product Z-Ala-OH. As shown in Figure S6D of the Supporting Information, a yield of no more than 60% Z-Ala-Gln was obtained when this ratio decreased below 2. In contrast, the yield of Z-Ala-Gln was as high as 70.0−71.5% when the G/Z ratio was between 3 and 4. This high yield of Z-Ala-OMe was significantly more than that obtained in previous studies.[13,42]

In general, in enzymatic dipeptide synthesis, a nucleophile such as Gln needs to be thoroughly dissolved in the reaction medium in the presence of a base, e.g., an organic base such as triethylamine (TEA). In the present study, 1.00 mmol TEA was necessary for complete dissolution of Gln. As illustrated in Figure S6E of the Supporting Information, the obtained yield of Z-Ala-Gln with PA@MNCC (from 71.5% to 64.4%) and free PA (from 66.3% to 57.6%) decreased gradually with increasing amounts of TEA from 1.00 to 1.60 mmol, because of the increased pH value of the reaction system and consequently the partial inactivation of the used enzyme. Clearly, the optimum amount of added TEA for the enzymatic synthesis of Z-Ala-Gln was shown to be 1.00 mmol. Within the examined amount of TEA, the observed yield of Z-Ala-Gln with PA@MNCC significantly surpassed its corresponding value with free PA, implying that PA@MNCC had a stronger resistance of deactivation in alkaline conditions than free PA, which was supported by the observation that PA@MNCC gave a relatively higher pH stability (Figure 6F).

The reusability of PA@MNCC is an important factor in its industrial application. As shown in Figure S6F of the Supporting Information, PA@MNCC retained more than 88% of its initial activity after use for 6 batches. Thus, PA@MNCC exhibited high reusability and great potential for enzymatic synthesis of Z-Ala-OMe.

Following the reaction, the dipeptide sample was subjected to LC-MS, and the result at m/z = 352.1515 $([M - H])^+$ confirmed that the product was Z-Ala-Gln (Figure S7 of the Supporting Information).

CONCLUSION

In conclusion, a novel biocompatible MNCC was successfully prepared by a simple coprecipitation-cross-linking technique for the first time. The as-prepared MNCC was shown to be a potential carrier for enzyme immobilization with high papain loading (333 mg/g MNCC) and high enzyme recovery (more than 80%). Moreover, papain immobilized on MCNC showed

DOI: 10.1021/acssuschemeng.5b00290
ACS Sustainable Chem. Eng. 2015, 3, 1589−1599

improved pH, thermal and storage stability than its free counterpart. A kinetic study and an apparent activation energy study for both PA@MNCC and free PA demonstrated that PA@MNCC had relatively higher catalytic efficiency and lower activation energy. Furthermore, the results of an application study illustrated that PA@MNCC had great potential in the biosynthesis of the Z-Ala-Gln dipeptide with a high yield in the novel DES green reaction medium. In addition, PA@MNCC showed good operational stability, which was supported by a reusability study that demonstrated that PA@MNCC retained more than 88% of its initial catalytic activity after being reused for 5 batches. Therefore, this work provides new prospects not only in the preparation of novel MNCC materials and the enzyme immobilization process but also in the application of the as-prepared PA@MNCC biocatalyst for the enzymatic synthesis of the important dipeptide, Z-Ala-Gln, in a DES reaction medium with a high yield.

■ ASSOCIATED CONTENT

Supporting Information

MNCC-6 (left) dispersed in aqueous solution and MNCC-6 attracted by external magnetic fields (right) (Figure S1). TGA analysis of NCC, Chitosan, and MNCC-4 (Figure S2). Effect of PA and MNCC mass ratio for enzyme immobilization (Figure S3). (A) Effect of GA mass fraction for enzyme immobilization; (B) effects of cross-linking time on the activity of immobilized papain (Figure S4). (A) Solvent tolerance of free PA and PA@MNCC; (B) structural integrity of free PA and PA@MNCC before and after reaction or exposure to CU-DES for 2 h. (Figure S5). Enzymatic synthesis of Z-Ala-Gln in DES-containing reaction system. (A) Effect of water content in DES; (B) effect of KCl concentration; (C) effect of reaction temperature; (D) effect of molar ratio of Gln to Z-Ala-OMe; (E) effect of TEA addition; (F) reuse of PA@MNCC in enzymatic synthesis of Z-Ala-OMe (Figure S6). UPLC-MS analysis of the synthesized product Z-Ala-Gln (Figure S7). The Supporting Information is available free of charge on the ACS Publications website at DOI: 10.1021/acssuschemeng.5b00290.

■ AUTHOR INFORMATION

Corresponding Author

*Prof. W.-Y. Lou. Tel.: +86-20-22236669. Fax: +86-20-22236669. E-mail: wylou@scut.edu.cn.

Notes

The authors declare no competing financial interest.

■ ACKNOWLEDGMENTS

We thank the National Natural Science Foundation of China (21336002; 21222606; 21376096), the Key Program of Guangdong Natural Science Foundation (S2013020013049), the National Key Basic Research Program of China (2013CB733500) and the Fundamental Research Funds for the Central Universities (2015PT002; 2015ZP009) for partially funding this work.

■ REFERENCES

(1) Sahoo, B.; Sahu, S. K.; Bhattacharya, D.; Dhara, D.; Pramanik, P. A novel approach for efficient immobilization and stabilization of papain on magnetic gold nanocomposites. *Colloids Surf., B. Biointerfaces* **2013**, *101*, 280−289.

(2) Fukuoka, A.; Dhepe, P. L. Catalytic conversion of cellulose into sugar alcohols. *Angew. Chem., Int. Ed.* **2006**, *45*, 5161−5163.

(3) Dutta, S.; De, S.; Alam, M. I.; Abu-Omar, M. M.; Saha, B. Direct conversion of cellulose and lignocellulosic biomass into chemicals and biofuel with metal chloride catalysts. *J. Catal.* **2012**, *288*, 8−15.

(4) Roy, D.; Semsarilar, M.; Guthrie, J. T.; Perrier, S. Cellulose modification by polymer grafting: A review. *Chem. Soc. Rev.* **2009**, *38*, 2046−2064.

(5) Xiong, R.; Zhang, X. X.; Tian, D.; Zhou, Z. H.; Lu, C. H. Comparing microcrystalline with spherical nanocrystalline cellulose from waste cotton fabrics. *Cellulose* **2012**, *19*, 1189−1198.

(6) Habibi, Y.; Lucia, L. A.; Rojas, O. J. Cellulose nanocrystals: Chemistry, self-assembly, and applications. *Chem. Rev.* **2010**, *110*, 3479.

(7) Incani, V.; Danumah, C.; Boluk, Y. Nanocomposites of nanocrystalline cellulose for enzyme immobilization. *Cellulose* **2013**, *20*, 191−200.

(8) Yang, R.; Tan, H.; Wei, F.; Wang, S. Peroxidase conjugate of cellulose nanocrystals for the removal of chlorinated phenolic compounds in aqueous solution. *Biotechnology* **2008**, *7*, 233−241.

(9) Edwards, J. V.; Prevost, N. T.; Condon, B.; French, A.; Wu, Q. Immobilization of lysozyme-cellulose amide-linked conjugates on cellulose I and II cotton nanocrystalline preparations. *Cellulose* **2012**, *19*, 495−506.

(10) Cao, S.-L.; Li, X.-H.; Lou, W.-Y.; Zong, M.-H. Preparation of a novel magnetic cellulose nanocrystal and its efficient use for enzyme immobilization. *J. Mater. Chem. B* **2014**, *2*, 5522−5530.

(11) Hartmann, R.; Meisel, H. Food-derived peptides with biological activity: From research to food applications. *Curr. Opin. Biotechnol.* **2007**, *18*, 163−169.

(12) Brosnan, J. T. Interorgan amino acid transport and its regulation. *J. Nutr.* **2003**, *133*, 2068S−2072S.

(13) Wang, M.; Qi, W.; Yu, Q.; Su, R.; He, Z. Kinetically controlled enzymatic synthesis of dipeptide precursor of L-alanyl−L-glutamine. *Biotechnol. Appl. Biochem.* **2011**, *58*, 449−455.

(14) Yagasaki, M.; Hashimoto, S. Synthesis and application of dipeptides; Current status and perspectives. *Appl. Microbiol. Biotechnol.* **2008**, *81*, 13−22.

(15) Furst, P. A thirty-year odyssey in nitrogen metabolism: From ammonium to dipeptides. *J. Parenter. Enteral Nutr.* **2000**, *24*, 197−209.

(16) Chen, F.; Zhang, F.; Wang, A.; Li, H.; Wang, Q.; Zeng, Z.; Wang, S.; Xie, T. Recent progress in the chemo-enzymatic peptide synthesis. *Afr. J. Pharm. Pharmacol.* **2010**, *4*, 721−730.

(17) Yazawa, K.; Numata, K. Recent advances in chemoenzymatic peptide syntheses. *Molecules* **2014**, *19*, 13755−13774.

(18) de Beer, R. J.; Zarzycka, B.; Mariman, M.; Amatdjais-Groenen, H., IV; Mulders, M. J.; Quaedflieg, P. J.; van Delft, F. L.; Nabuurs, S. B.; Rutjes, F. P. Papain-specific activating esters in aqueous dipeptide synthesis. *ChemBioChem* **2012**, *13*, 1319−1326.

(19) Noritomi, H.; Suzuki, K.; Kikuta, M.; Kato, S. Catalytic activity of A-chymotrypsin in enzymatic peptide synthesis in ionic liquids. *Biochem. Eng. J.* **2009**, *47*, 27−30.

(20) Salam, S. M. A.; Kagawa, K.-i.; Matsubara, T.; Kawashiro, K. Protease-catalyzed dipeptide synthesis from N-protected amino acid carbamoylmethyl esters and free amino acids in frozen aqueous solutions. *Enzyme Microb. Technol.* **2008**, *43*, 537−543.

(21) Nuijens, T.; Cusan, C.; van Dooren, T. J.; Moody, H. M.; Merkx, R.; Kruijtzer, J. A.; Rijkers, D. T.; Liskamp, R. M.; Quaedflieg, P. J. Fully enzymatic peptide synthesis using C-terminal tert-butyl ester interconversion. *Adv. Synth. Catal.* **2010**, *352*, 2399−2404.

(22) Abbott, A. P.; Capper, G.; Davies, D. L.; Rasheed, R. K.; Tambyrajah, V. Novel solvent properties of choline chloride/urea mixtures. *Chem. Commun.* **2003**, 70−71.

(23) Durand, E.; Lecomte, J.; Villeneuve, P. Deep eutectic solvents: Synthesis, application, and focus on lipase-catalyzed reactions. *Eur. J. Lipid Sci. Technol.* **2013**, *115*, 379−385.

(24) Bondeson, D.; Mathew, A.; Oksman, K. Optimization of the isolation of nanocrystals from microcrystalline cellulose by acid hydrolysis. *Cellulose* **2006**, *13*, 171−180.

(25) Cao, S. L.; Lou, W. Y.; Zong, M. H. Preparation of novel magnetic cellulose nanocrystals via in-situ co-precipitation-electrostatic self-assembly technique and its efficient use for enzyme immobilization. *J. Mater. Chem. B* **2014**, *2*, 5522−5530.
(26) Gawande, M. B.; Velhinho, A.; Nogueira, I. D.; Ghumman, C.; Teodoro, O.; Branco, P. S. A facile synthesis of cysteine−ferrite magnetic nanoparticles for application in multicomponent reactions—A sustainable protocol. *RSC Adv.* **2012**, *2*, 6144−6149.
(27) Nissen, M. S.; Kumar, G. M.; Youn, B.; Knowles, D. B.; Lam, K. S.; Ballinger, W. J.; Knowles, N. R.; Kang, C. Characterization of *Solanum tuberosum* multicystatin and its structural comparison with other cystatins. *Plant Cell* **2009**, *21*, 861−875.
(28) Brugnerotto, J.; Lizardi, J.; Goycoolea, F. M.; Arguelles-Monal, W.; Desbrieres, J.; Rinaudo, M. An infrared investigation in relation with chitin and chitosan characterization. *Polymer* **2001**, *42*, 3569−3580.
(29) Leung, A. C.; Hrapovic, S.; Lam, E.; Liu, Y.; Male, K. B.; Mahmoud, K. A.; Luong, J. H. Characteristics and properties of carboxylated cellulose nanocrystals prepared from a novel one-step procedure. *Small* **2011**, *7*, 302−305.
(30) Liu, Z.; Wang, H.; Li, B.; Liu, C.; Jiang, Y.; Yu, G.; Mu, X. Biocompatible magnetic cellulose-chitosan hybrid gel microspheres reconstituted from ionic liquids for enzyme immobilization. *J. Mater. Chem.* **2012**, *22*, 15085−15091.
(31) Vieira, R. S.; Meneghetti, E.; Baroni, P.; Guibal, E.; González de la Cruz, V. M.; Caballero, A.; Rodríguez-Castellón, E.; Beppu, M. M. Chromium removal on chitosan-based sorbents−An EXAFS/XANES investigation of mechanism. *Mater. Chem. Phys.* **2014**, *146*, 412−417.
(32) Chen, H.-L.; Yokochi, A. X-ray diffractometric study of microcrystallite size of naturally colored cottons. *J. Appl. Polym. Sci.* **2000**, *76*, 1466−1471.
(33) Qi, L.; Xu, Z.; Jiang, X.; Hu, C.; Zou, X. Preparation and antibacterial activity of chitosan nanoparticles. *Carbohydr. Res.* **2004**, *339*, 2693−2700.
(34) Xu, H.; Tong, N.; Cui, L.; Lu, Y.; Gu, H. Preparation of hydrophilic magnetic nanospheres with high saturation magnetization. *J. Magn. Magn. Mater.* **2007**, *311*, 125−130.
(35) Wang, Y.; Li, B.; Zhou, Y.; Jia, D. Chitosan-induced synthesis of magnetite nanoparticles via iron ions assembly. *Polym. Adv. Technol.* **2008**, *19*, 1256−1261.
(36) de Mesquita, J. P.; Donnici, C. L.; Pereira, F. V. Biobased nanocomposites from layer-by-layer assembly of cellulose nanowhiskers with chitosan. *Biomacromolecules* **2010**, *11*, 473−480.
(37) Mahmoud, K. A.; Lam, E.; Hrapovic, S.; Luong, J. H. Preparation of well-dispersed gold/magnetite nanoparticles embedded on cellulose nanocrystals for efficient immobilization of papain enzyme. *ACS Appl. Mater. Interfaces* **2013**, *5*, 4978−4985.
(38) Aytar, B. S.; Bakir, U. Preparation of cross-linked tyrosinase aggregates. *Process Biochem.* **2008**, *43*, 125−131.
(39) Kumar, S.; Mohan, U.; Kamble, A. L.; Pawar, S.; Banerjee, U. C. Cross-linked enzyme aggregates of recombinant *Pseudomonas putida* nitrilase for enantioselective nitrile hydrolysis. *Bioresour. Technol.* **2010**, *101*, 6856−6858.
(40) Talekar, S.; Ghodake, V.; Ghotage, T.; Rathod, P.; Deshmukh, P.; Nadar, S.; Mulla, M.; Ladole, M. Novel magnetic cross-linked enzyme aggregates (magnetic CLEAs) of alpha amylase. *Bioresour. Technol.* **2012**, *123*, 542−547.
(41) Montoro-García, S.; Gil-Ortiz, F.; Navarro-Fernández, J.; Rubio, V.; García-Carmona, F.; Sánchez-Ferrer, Á. Improved cross-linked enzyme aggregates for the production of desacetyl β-lactam antibiotics intermediates. *Bioresour. Technol.* **2010**, *101*, 331−336.
(42) Wang, M.; Qi, W.; Yu, Q.; Su, R.; He, Z. Cross-linking enzyme aggregates in the macropores of silica gel: A practical and efficient method for enzyme stabilization. *Biochem. Eng. J.* **2010**, *52*, 168−174.
(43) Lei, H.; Wang, W.; Chen, L. L.; Li, X. C.; Yi, B.; Deng, L. The preparation and catalytically active characterization of papain immobilized on magnetic composite microspheres. *Enzyme Microb. Technol.* **2004**, *35*, 15−21.
(44) Chiou, S.-H.; Wu, W.-T. Immobilization of *Candida rugosa* lipase on chitosan with activation of the hydroxyl groups. *Biomaterials* **2004**, *25*, 197−204.
(45) Sangeetha, K.; Emilia Abraham, T. Preparation and characterization of cross-linked enzyme aggregates (CLEA) of subtilisin for controlled release applications. *Int. J. Biol. Macromol.* **2008**, *43*, 314−319.
(46) Yu, C.-Y.; Li, X.-F.; Lou, W.-Y.; Zong, M.-H. Cross-linked enzyme aggregates of mung bean epoxide hydrolases: A highly active, stable and recyclable biocatalyst for asymmetric hydrolysis of epoxides. *J. Biotechnol.* **2013**, *166*, 12−19.
(47) Lyu, F.; Zhang, Y.; Zare, R. N.; Ge, J.; Liu, Z. One-pot synthesis of protein-embedded metal-organic frameworks with enhanced biological activities. *Nano Lett.* **2014**, *14*, 5761−5765.
(48) Susanti, D.; Suhartati, T.; Hadi, S. Immobilization of α-amylase from locale bacteria isolate *Bacillus subtilis* ITBCCB148 with carboxymethyl cellulose (CM-cellulose). *Modern Appl. Sci.*, **2012**, *6*.
(49) Yang, Z.; Domach, M.; Auger, R.; Yang, F. X.; Russell, A. J. Polyethylene glycol-induced stabilization of Subtilisin. *Enzyme Microb. Technol.* **1996**, *18*, 82−89.
(50) Byler, D. M.; Wilson, R. M.; Randall, C. S.; Sokoloski, T. D. Second derivative infrared spectroscopy as a non-destructive tool to assess the purity and structural integrity of proteins. *Pharm. Res.* **1995**, *12*, 446−450.
(51) Natalello, A.; Ami, D.; Brocca, S.; Lotti, M.; Doglia, S. Secondary structure, conformational stability and glycosylation of a recombinant *Candida rugosa* lipase studied by Fourier-transform infrared spectroscopy. *Biochem. J.* **2005**, *385*, 511−517.
(52) Lou, W.-Y.; Zong, M.-H.; Smith, T. J.; Wu, H.; Wang, J.-F. Impact of ionic liquids on papain: An investigation of structure−function relationships. *Green Chem.* **2006**, *8*, 509−512.
(53) Vecchio, G.; Zambianchi, F.; Zacchetti, P.; Secundo, F.; Carrea, G. Fourier-transform infrared spectroscopy study of dehydrated lipases from *Candida antarctica* B and *Pseudomonas cepacia*. *Biotechnol. Bioeng.* **1999**, *64*, 545−551.
(54) Collins, M. D.; Quillin, M. L.; Hummer, G.; Matthews, B. W.; Gruner, S. M. Structural rigidity of a large cavity-containing protein revealed by high-pressure crystallography. *J. Mol. Biol.* **2007**, *367*, 752−763.
(55) Zaks, A.; Klibanov, A. M. Enzymatic catalysis in nonaqueous solvents. *J. Biol. Chem.* **1988**, *263*, 3194−3201.
(56) Klibanov, A. M. Improving enzymes by using them in organic solvents. *Nature* **2001**, *409*, 241−246.
(57) Danson, M. J.; Hough, D. W. Structure, function and stability of enzymes from the archaea. *Trends Microbiol.* **1998**, *6*, 307−314.
(58) Maugeri, Z.; Leitner, W.; de Maria, P. D. Chymotrypsin-catalyzed peptide synthesis in deep eutectic solvents. *Eur. J. Org. Chem.* **2013**, *2013*, 4223−4228.
(59) Otzen, D. E. Protein unfolding in detergents: Effect of micelle structure, ionic strength, pH, and temperature. *Biophys. J.* **2002**, *83*, 2219−2230.

DOI: 10.1021/acssuschemeng.5b00290
ACS Sustainable Chem. Eng. 2015, 3, 1589−1599